

Surface currents on models of force-free solar magnetic flux tubes

By **D. B. MELROSE, JENNIFER NICHOLLS**
AND **N. G. BRODERICK**

Research Centre for Theoretical Astrophysics, University of Sydney,
NSW 2006, Australia

(Received 4 December 1993 and in revised form 12 January 1994)

A model of a cylindrically symmetric, force-free magnetic field consisting of a sequence of concentric layers with piecewise-constant α is used to construct models of the surface currents on isolated, force-free magnetic flux tubes. Two boundary conditions are considered: a current-neutralized flux tube ($B_\phi = 0$, $B_z \neq 0$ at $r > r_0$), and an isolated current-carrying flux tube ($B_\phi \neq 0$, $B_z = 0$ at $r > r_0$). A single- α model that is current-neutralized is a reverse-field pinch, and is unacceptable as a model for a solar flux tube. Examples of two- α models for a current-neutralized flux tube are presented. The models of the surface currents satisfying either boundary condition are shown to simplify considerably when the surface layer is thin. A model consisting of several layers, with piecewise-constant α , may be used to find an approximate solution for a force-free flux tube with an arbitrarily specified current profile.

1. Introduction

Solar magnetic flux tubes are usually modelled as isolated, twisted, force-free structures (see e.g. Bray et al. 1991). The arguments for treating flux tubes as isolated structures are partly observational, with flux tubes in the photosphere appearing to act as isolated entities (see e.g. Parker 1979, p. 123), and partly for mathematical convenience (see e.g. Priest 1982, p. 108). Twists and shears imply a current, and the force-free assumption, relevant to the low- β plasma in the corona, requires that the current density \mathbf{J} be along the magnetic field, \mathbf{B} . However, the outer boundary condition on such a flux tube has been given relatively little attention. Consider a cylindrical flux tube of radius r_0 . Three different boundary conditions might be contemplated.

(a) A completely isolated *flux* tube such that the magnetic field is zero outside the cylinder: $\mathbf{B} = 0$ at $r \geq r_0$. However, this is not possible, because, as pointed out by Gold & Hoyle (1960), this boundary condition is incompatible with the force-free assumption.

(b) A current-neutralized flux tube such that there is a uniform axial field outside the cylinder: $B_z = \text{const}$ at $r \geq r_0$. This boundary condition would apply, for example, to a model in which a twisting motion is imposed at $r < r_0$ on a pre-existing uniform field. Such an idealized twist involves an axial current flowing in one direction inside the cylinder and a neutralizing return current flowing on the surface of the cylinder (see e.g. Chiuderi et al. 1980).

(c) An isolated current-carrying flux tube such that there is a purely azimuthal

field outside the cylinder: $B_\phi \propto 1/r$ at $r \geq r_0$. This boundary condition also requires a surface current if the interior solution has $B_z(r_0) \neq 0$.

A more general question arises in connection with boundary conditions (b) or (c): can a force-free surface current be constructed to satisfy either (b) or (c) for any given force-free solution at $r < r_0$? Recently Low (1993) presented one specific model for a surface current satisfying boundary condition (c). In this paper we present a simple technique that enables one to construct a force-free surface current satisfying either boundary condition in a cylinder shell of arbitrary thickness.

The force-free condition may be written in the form $\mu_0 \mathbf{J}(\mathbf{x}) = \alpha(\mathbf{x}) \mathbf{B}(\mathbf{x})$. We consider models in which $\alpha(r)$ is a piecewise-constant function of radius r . We discuss three different uses for such constant- α models: to construct exact solutions with one or more regions of constant α , to construct force-free surface currents that satisfy boundary conditions (b) or (c) above for any given interior solution, and to construct approximate solutions for any given current profile by approximating that profile by a sequence of piecewise constant current shells. The single- α model is well known: it is the Lundquist solution, $B_\phi = B_0 J_1(\alpha r)$, $B_z = B_0 J_0(\alpha r)$, where B_0 is a constant and J_n is a Bessel function. An outer boundary condition is required, and either (b) or (c) can be imposed simply. If one imposes boundary condition (b) then a solution exists with αr_0 corresponding to the first non-trivial zero of J_0 . This solution is referred to as a *reverse-field pinch*, where 'reverse-field' refers to the change in sign of B_z at the first zero of J_0 , which occurs at $r < r_0$. Alternatively, if one imposes boundary condition (c) then a solution exists with αr_0 corresponding to the first zero of J_1 . There are arguments for (see e.g. Taylor 1974, 1986; Norman & Heyvaerts 1983; Heyvaerts & Priest 1984; Browning, Sakurai & Priest 1986) and against (see e.g. Low 1985) a single- α model for solar magnetic fields. With boundary condition (b), a strong argument against a reverse-field pinch model is that solar magnetic flux tubes have a non-zero magnetic flux, $\Phi_M \neq 0$, whereas a single- α model has $\mathbf{I} = \alpha \Phi_M \mathbf{e}_z$, where \mathbf{I} is the axial current, and $\mathbf{I} = 0$ in a reverse-field pinch would imply $\Phi_M = 0$. Here we show that one can construct two- α models with $\mathbf{I} = 0$ and $\Phi_M \neq 0$ that satisfy boundary condition (b); such models have $\alpha = \alpha_1$ at $r < r_1$, and $\alpha = \alpha_2$ at $r_1 < r < r_2$, where the outer boundary is now $r = r_2$. Moreover, similar to the outer region in a two- α model, one may construct a force-free surface region that satisfies either boundary condition (b) or (c) for an arbitrary (non-constant- α) interior solution.

The matching condition at the boundary between the two regions in a two- α model also applies to the boundary between any two regions in a multi- α model. Such a model may be used to approximate any current distribution to arbitrary accuracy by including a sufficiently large number of constant- α shells. The main advantage of such an approach is that it enables one to calculate, using simple functions (Bessel functions), the magnetic field for a given force-free current profile to any desired accuracy. This is to be compared with an alternative approach in which a general class of cylindrically symmetric, force-free solutions is written down in terms of a generating function $f(r)$, with $B_\phi^2 = -\frac{1}{2} r f'$, $B_z^2 = f + \frac{1}{2} r f'$, $f' = df/dr$ (Lust & Schluter 1954). The implied current profile corresponds to $\alpha = -(3f' + r f'')/4[(\frac{1}{2} r f')^2 + (f + \frac{1}{2} r f')^2]^{\frac{1}{2}}$, which cannot readily be inverted to find f . That is, it is not straightforward to find the generating function corresponding to a given current profile. In contrast, the

piecewise-constant-a model provides a relatively simple way of constructing an approximate solution for any given current profile.

In §2 we show examples of two-a models. In §3 we show how a surface layer satisfying either boundary condition (b) or (c) may be constructed, and then concentrate on the case where this layer is arbitrarily thin, corresponding to a singular surface current. In §4 we illustrate how the piecewise-constant-a model may be used to approximate some known solutions, to establish its usefulness in constructing solutions for any other given current profile.

2. The two-a model

A static constant-a field is defined as a magnetic field that satisfies

$$\text{curl } \mathbf{B} = \alpha \mathbf{B}. \quad (1)$$

In terms of cylindrical polar co-ordinates (r, ϕ, z) , a solution of (1) exists in terms of Bessel functions:

$$\left. \begin{aligned} B_\phi(r) &= aJ_1(\alpha r) + bY_1(\alpha r), \\ B_z(r) &= aJ_0(\alpha r) + bY_0(\alpha r), \end{aligned} \right\} \quad (2)$$

where a and b are constants. In a multi-a model we have n concentric regions, with the outer radius of the i th shell at r_i and with $a = \alpha_i$ in the i th shell. Although we are concerned with the case $n = 2$ in this section, it is convenient to treat the case of arbitrary n in setting up the problem. The requirement that B be finite at $r = 0$ then gives

$$\mathbf{B} = \begin{cases} (0, B_0 J_1(\alpha_1 r), B_0 J_0(\alpha_1 r)) & (0 \leq r \leq r_1), \\ (0, a_i J_1(\alpha_i r) + b_i Y_1(\alpha_i r), a_i J_0(\alpha_i r) + b_i Y_0(\alpha_i r)) & (r_{i-1} \leq r \leq r_i), \end{cases} \quad (3)$$

with $i = 2, \dots, n$. We seek a solution such that B is continuous at each $r = r_i$. The matching condition at $r = r_1$ reduces to

$$\begin{pmatrix} J_1(\alpha_2 r_1) & Y_1(\alpha_2 r_1) \\ J_0(\alpha_2 r_1) & Y_0(\alpha_2 r_1) \end{pmatrix} \begin{pmatrix} a_2 \\ b_2 \end{pmatrix} = B_0 \begin{pmatrix} J_1(\alpha_1 r_1) \\ J_0(\alpha_1 r_1) \end{pmatrix}. \quad (4)$$

A solution exists for

$$\begin{vmatrix} J_1(\alpha_2 r_1) & Y_1(\alpha_2 r_1) \\ J_0(\alpha_2 r_1) & Y_0(\alpha_2 r_1) \end{vmatrix} \neq 0, \quad (5)$$

which is always satisfied because the zeros of different Bessel functions do not coincide. In the same way, one finds that the matching condition at each r_i with $i > 2$ is also satisfied. Thus one may construct an arbitrary piecewise-constant-a model with no need for singular currents at any of the internal radii, r_i where different solutions are matched.

2.1. Boundary conditions

We discuss two boundary conditions, designated as (b) and (c) above. Case (b) corresponds to a solution with zero net current. For an n -a model the axial current is given by

$$I = 2\pi \int_0^{r_n} dr r J_z(r) = \frac{2\pi r_n}{\mu_0} B_\phi(r_n), \quad (6)$$

where Ampère's equation has been used. The condition $\mathbf{I} = \mathbf{0}$ then reduces to $B_\phi(r_n) = 0$, and with (3) this becomes

$$a_n J_1(\alpha_n r_n) + b_n Y_1(\alpha_n r_n) = 0. \quad (7)$$

Outside the cylinder there is a uniform axial field; that is, $B_\phi(r) = 0$, $B_z = \text{const}$ at $r \geq r_n$.

The other boundary condition (c) requires $B_r = 0$ at $r \geq r_n$. This can be satisfied with a single-a model by locating the surface at r_0 such that αr_0 is the first zero of J_0 . We do not discuss this case further in this section.

2.2. Special cases

Before presenting specific two-a solutions, it is appropriate to discuss two special cases: the weak-current limit and the reverse-field pinch.

The weak-current limit corresponds to $|\alpha_1|r_1 \ll 1$ and $|\alpha_2|$ not too large. Then each Bessel function may be approximated by the leading term in its power-series expansion. As a result, $B_\phi < B_z$, with $B_z \approx B_0$. In this limit

$$B_\phi(r) = \frac{\mu_0 I(r)}{2\pi r}, \quad I(r) = \begin{cases} \frac{\pi B_0}{r} \alpha_1 r^2 & (r < r_1), \\ \frac{\pi B_0}{r} \alpha_1 r_1^2 + \alpha_2 (r^2 - r_1^2) & (r_1 < r < r_2). \end{cases} \quad (8)$$

The condition $\mathbf{I} = I(r_2) = 0$ then reduces to $\alpha_2/\alpha_1 = -r_1^2/(r_2^2 - r_1^2)$. The power-series expansion of the Bessel functions in the outer region is valid only for $|\alpha_2|r_2 \ll 1$, which excludes cases with $r_2 - r_1 \ll r_1$; that is, it is not valid for a nearly singular return current on the surface of the cylinder.

In any model with axial symmetry a given magnetic field line is confined to the surface of a cylinder at constant r . The field lines wind around the cylinder with a constant pitch, described by the pitch angle

$$\tan \theta(r) = \frac{B_\phi(r)}{B_z(r)}. \quad (9)$$

Our choice of ϑ is such that $\theta = 0$ corresponds to an untwisted, axial field line, and $\vartheta = \frac{1}{2}\pi$ corresponds to field lines that are circles centred on the axis. In the weak-current limit the pitch angle is always small.

For larger values of r_1 the field in the inner region differs significantly from the weak-current limit. In models with $|\alpha_1|r_1 > 2.40$, where $z = 2.40$ corresponds to the first zero of $J_0(z)$, the direction of both the axial magnetic field and the axial current reverse within the inner region. In such models the pitch angle increases, with $\vartheta = \frac{1}{2}\pi$ at the first zero of J_0 . Such a model becomes a reverse-field pinch for $|\alpha_1|r_1 = 3.83$, where $z = 3.83$ corresponds to the first non-trivial zero of $J_1(z)$, and then boundary condition (b) is satisfied for $r_2 = r_1$, that is, for a single-a model. A two-a model that satisfies boundary condition (b) is of interest for $|\alpha_1|r_1$ not small enough for the weak-current limit to be satisfied, but with $|\alpha_1|r_1 < 2.40$, so that the current neutralization is provided by the outer region, $r_1 < r < r_2$.

2.3. Current-neutralized two-a solutions

The procedure used here to construct models of force-free fields is as follows. First, dimensionless parameters are introduced. The magnitude of the magnetic field is arbitrary, and is fixed by setting $B_0 = 1$. The parameters a , and a , have

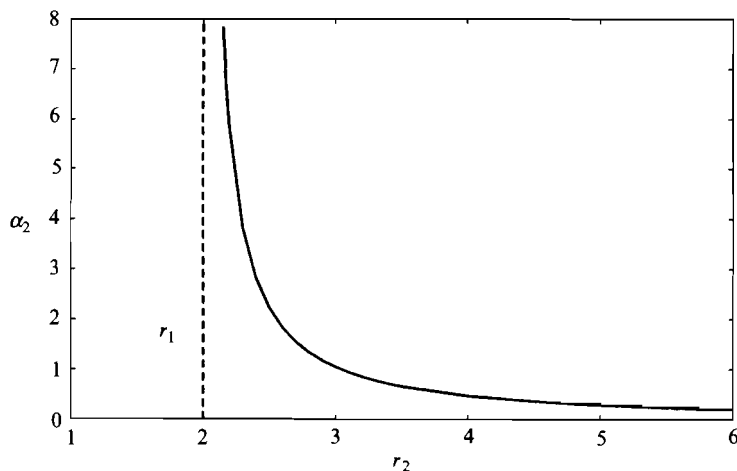


FIGURE 1. The solution for a , as a function of r_2 for $r_1 = 2$

the dimensions of inverse lengths, and setting $|\alpha_1| = l$ fixes the scale length. (For convenience, we choose a , to be negative, so the scale length is actually defined by setting $a = -l$.) Different models may be described in terms of three dimensionless parameters $\bar{r}_1 = |\alpha_1|r_1$, $\bar{r}_2 = |\alpha_1|r_2$ and $\bar{\alpha}_2 = \alpha_2/|\alpha_1|$. In the remainder of this section the bars are omitted on these parameters. A particular model is constructed by choosing r_1 and r . Equation (4) is inverted to find a and b in terms of the Bessel functions, and the resulting expressions for a and b are substituted into (7), which is solved numerically for a . The smallest solution for a , is chosen; if any other solution is chosen then there is a reversal in the axial field component B_z , as occurs in a reverse-field pinch. The assumption that there is no reversal of the axial magnetic field in the inner region implies that a , and a , are necessarily of opposite sign, in order that the currents in the two regions be in opposite directions so that they can neutralize each other. The choice $a = -l$ then implies that a , is positive. Once a , is found, the full solution is constructed.

A wide range of models is possible, depending on the choices of r_1 and r_2 . As noted above, $r_1 \ll l$ corresponds to the weak-current limit, and for $r_1 > 2.40$ bur model approaches a reverse-field pinch. In figure 1 we illustrate a case with $r_1 = 2$, in which the current is not weak and in which there is no reversal of the axial magnetic field. The minimum value of r_2 allowed in the model is $r_2 = r_1$, which is indicated in figure 1 by the dashed line. The general form of the solution found in figure 1 may be understood as follows. In the limit as $r_2 \rightarrow r_1$ the ratio of the areas of the outer and inner regions approaches zero, and because boundary condition (b) requires that the two regions carry equal and opposite currents, the ratio of the current densities approaches infinity, implying $a, \rightarrow \infty$. In this limit ($r_2 - r_1 \rightarrow 0$) the current in the outer region corresponds to a singular return current on the surface of the flux tube. For $r_2 \rightarrow \infty$ the ratio of the areas approaches infinity, and hence the ratio of the current densities approaches zero, implying $a, \rightarrow 0$.

To complement the solution plotted in figure 1 for one specific value $r_1 = 2$, the solution for a , is plotted as a function of r_1 in figure 2 for a fixed value of

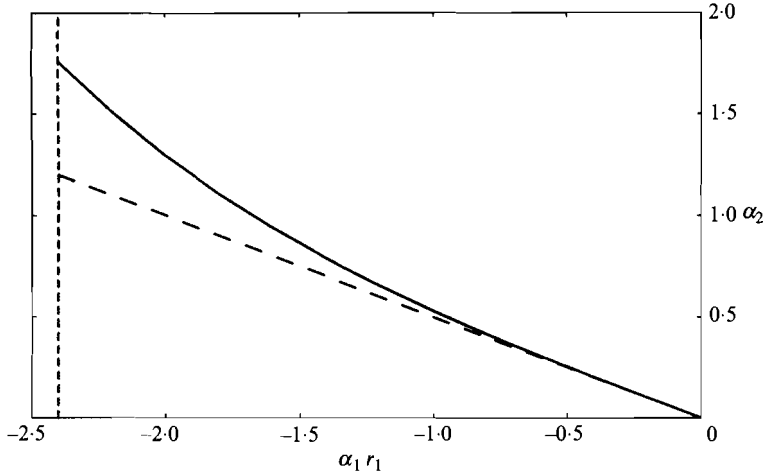


FIGURE 2. The solution for α , versus r_1 (—) for $r_2 = 2^{1/2}r_1$; the weak-current limit (---) is shown for comparison.

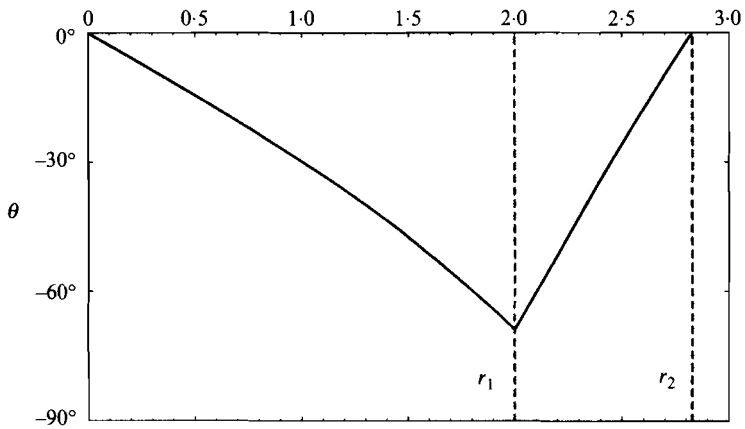


FIGURE 3. The pitch angle θ as a function of radius for $r_1 = 2$ and $r_2 = 2^{1/2}$.

the ratio r_2/r_1 . The value chosen, $r_2/r_1 = 2^{1/2}$, corresponds to equal areas for the inner and outer regions. In this case, to emphasize that \mathbf{a} , and \mathbf{a} , have opposite signs, we plot \mathbf{a} , versus \mathbf{a} , $r_1 = -r_1$. The solid line shows the dependence of \mathbf{a} , on r_1 in the model, and for comparison the dashed line shows the dependence of \mathbf{a} , on r_1 in the weak-current limit. The vertical dashed line at -2.40 indicates the value of r_1 beyond which B_z changes sign as the reverse-field pinch configuration is approached.

The pitch angle is plotted as a function of radius for a two- \mathbf{a} model in figure 3. The parameters chosen are $r_1 = 2$ and equal areas for the inner and outer regions ($r_2 = 2^{1/2}r_1$). The pitch angle θ , which is negative because of our choice \mathbf{a} , $= -1$, decreases with radius from zero at $r = 0$ to a minimum at r_1 , and then increases with increasing radius back to zero at r_2 . The pitch angle approaches zero at r_2 because of our requirement that the net current be zero: Ampère's law then implies that the field lines at $r \geq r_2$ are straight. For other choices of r_1 the

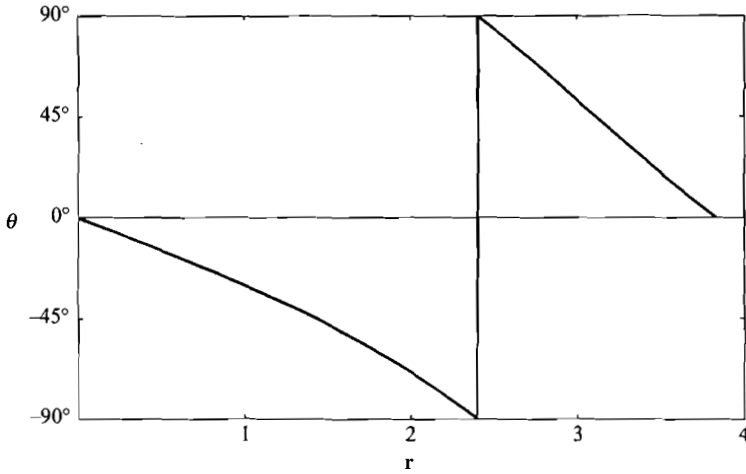


FIGURE 4. The pitch angle θ as a function of radius for a reverse-field pinch

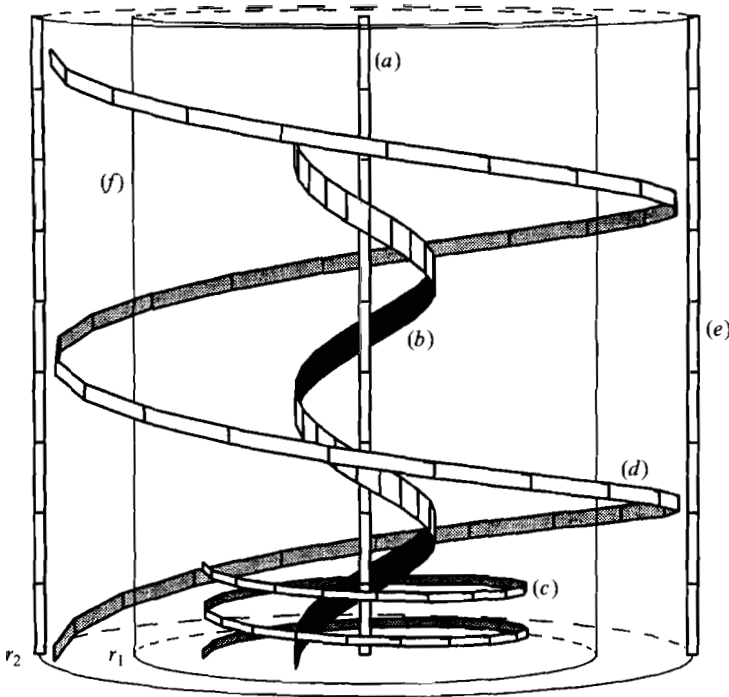


FIGURE 5. Representative magnetic field lines (a)-(e) for the two-a model of figure 3. Each field line is followed for a twist through 4π .

form of the solution is similar to that illustrated in figure 3: the minimum value of θ decreases with increasing r_1 , and for $r_1 = 2.40$ the minimum value is $\theta = -\frac{1}{2}\pi$. For $r_1 > 2.40$, after relabelling $\theta = -\frac{1}{2}\pi \rightarrow \theta = +\frac{1}{2}\pi$, we have $\theta < \frac{1}{2}\pi$ in the region $2.40 < r < r_1$, corresponding to a twist in the opposite direction due to a reversal in the sign of the axial magnetic field, as in a reverse-field pinch. For comparison, a reverse-field pinch is shown in figure 4: θ decreases with radius from zero at $r = 0$ to $-\frac{1}{2}\pi$ at the first zero of J_0 at $r = 2.40$, where the axial field

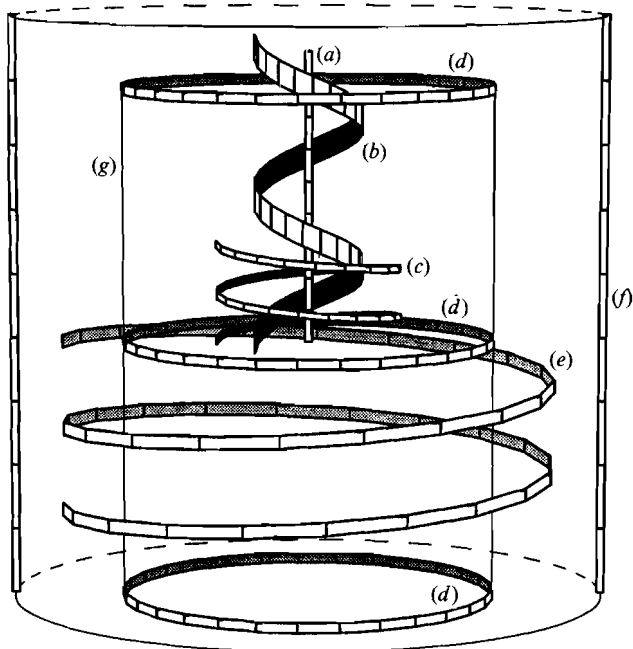


FIGURE 6. As in figure 5, but for a reverse-field pinch

changes sign. The pitch angle reaches $\beta = 0$ at $r = 3.83$, which is the first non-trivial zero of J_z , this being the maximum radius in a reverse-field pinch (see e.g. Taylor 1986).

2.4. Plots of two- α solutions

The results of numerical calculations of a two- α model with zero net current are illustrated in figure 5. Representative magnetic field lines (a)–(e) are shown in three dimensions for the case with $\alpha = -1$, $r_1 = 2$ and $r_2 = 2\frac{1}{2}r_1$ (implying $\alpha = 1.3$). Field lines are plotted as ribbons, and the other lines in the figure are to guide the eye. The field line (a) at $r = 0$ is straight, corresponding to $\beta = 0$. As the radius increases, $|\theta|$ increases (β is negative) as illustrated in (b) and (c). Each field line is plotted to the height reached after two complete rotations about the cylinder, that is, a twist through 4π . At r_1 , indicated by the cylinder (f), $|\theta|$ has its maximum value, which is less than $\frac{1}{2}\pi$ here owing to the choice of $r_1 < 2.40$. For $r > r_1$, $|\theta|$ decreases, as shown by (d), until at $r = r_2$, we have $\beta = 0$ and the outermost field lines (e) are straight.

Figure 6 is similar to figure 5, but for a single- α model with zero net current, which corresponds to a reverse-field pinch. The field line (a) is straight, and $|\theta|$ increases with radius as shown in (b) and (c). At $r = 2.40$, we have $B_z = 0$, $J_0 = 0$, so the field is entirely in the ϕ direction ($\beta = -\frac{1}{2}\pi$), as indicated by the three circles labelled (d). As the radius increases from this value, J_0 becomes negative, and the axial component of the magnetic field reverses its direction, as shown by (e). A further increase in the radius causes an increase in $|\theta|$ to more than $\frac{1}{2}\pi$ owing to B_z , having changed sign (see figure 4), until at $r = 3.83$, which is the first non-trivial zero of J_z , the outermost field lines (f) are straight ($|\theta| = \pi$).

Note the qualitative difference between the two- α model (figure 5), in which the sign of B_z does not change, so that the net magnetic flux is non-zero, and

the reverse-field pinch (figure 6), in which the sign of B_z changes at an intermediate radius, so that the net magnetic flux is zero. (The net current is zero in both models by construction.) As a consequence, in the two- a model the sense of the twist is always the same ($|\theta| < \frac{1}{2}\pi$), whereas in a reverse-field pinch the sense of the twist reverses where B_z passes through zero.

3. Surface currents

The solution (3) in the region $r_1 < r < r_2$ may be used to construct a force-free surface current for any values of B_ϕ and B_z at $r \leq r_1$. This surface current may be chosen to satisfy either of our two alternative boundary conditions, and it simplifies greatly in the limit of a thin surface.

3.1. General matching condition

On matching the solution (3) to arbitrary values of B_ϕ and B_z at $r = r_1$, one finds

$$B_\phi(r) = \frac{1}{J_0(\alpha_2 r_1) Y_1(\alpha_2 r_1) - J_1(\alpha_2 r_1) Y_0(\alpha_2 r_1)} \\ \times \{ -B_\phi(r_1) [J_1(\alpha_2 r) Y_0(\alpha_2 r_1) - Y_1(\alpha_2 r) J_0(\alpha_2 r_1)] \\ + B_z(r_1) [J_1(\alpha_2 r) Y_1(\alpha_2 r_1) - Y_1(\alpha_2 r) J_1(\alpha_2 r_1)] \}, \quad (10)$$

$$B_z(r) = \frac{1}{J_0(\alpha_2 r_1) Y_1(\alpha_2 r_1) - J_1(\alpha_2 r_1) Y_0(\alpha_2 r_1)} \\ \times \{ -B_\phi(r_1) [J_0(\alpha_2 r) Y_0(\alpha_2 r_1) - Y_0(\alpha_2 r) J_0(\alpha_2 r_1)] \\ + B_z(r_1) [J_0(\alpha_2 r) Y_1(\alpha_2 r_1) - Y_0(\alpha_2 r) J_1(\alpha_2 r_1)] \}. \quad (11)$$

One can always find a value of a , r_2 to satisfy either our boundary condition (b) $B_\phi(r_2) = 0$ or our boundary condition (c) $B_z(r_2) = 0$.

3.2. Thin surface-current layers

Considerable simplification occurs if the surface layer is thin, $r_2 - r_1 \ll r_1$, so that $|\alpha_2 r_1|$ is large. The Bessel functions may then be approximated by their asymptotic forms

$$\left. \begin{aligned} J_\nu(z) &\approx \left(\frac{2}{\pi z}\right)^{\frac{1}{2}} \cos\left(z - \frac{1}{2}\nu\pi - \frac{1}{4}\pi\right), \\ Y_\nu(z) &\approx \left(\frac{2}{\pi z}\right)^{\frac{1}{2}} \sin\left(z - \frac{1}{2}\nu\pi - \frac{1}{4}\pi\right) \end{aligned} \right\} \quad (12)$$

which apply for $|\alpha_2 r_1| \gg 1$. The solutions (10) and (11) then reduce to

$$B_\phi(r) = B_\phi(r_1) \cos[\alpha_2(r - r_1)] + B_z(r_1) \sin[\alpha_2(r - r_1)], \quad (13)$$

$$B_z(r) = -B_\phi(r_1) \sin[\alpha_2(r - r_1)] + B_z(r_1) \cos[\alpha_2(r - r_1)]. \quad (14)$$

Now imposing the boundary condition (b) $B_\phi(r_2) = 0$ on (13) gives

$$\left. \begin{aligned} B_\phi(r) &= B_\phi(r_1) \frac{\sin[\alpha_2(r_2 - r)]}{\sin[\alpha_2(r_2 - r_1)]}, \\ B_z(r) &= B_z(r_1) \frac{\cos[\alpha_2(r_2 - r)]}{\cos[\alpha_2(r_2 - r_1)]} \end{aligned} \right\} \quad (15)$$

which requires that $\alpha_2(r_2 - r_1)$ satisfy

$$\tan[\alpha_2(r_2 - r_1)] = -\frac{B_\phi(r_1)}{B_z(r_1)}. \quad (16)$$

One has $B_\phi = 0$, $B_z = \text{const}$ at $r > r_2$.

Alternatively, imposing the boundary condition (c) on (14), $B_z(r_2) = 0$ gives

$$\left. \begin{aligned} B_\phi(r) &= B_\phi(r_1) \frac{\cos[\alpha_2(r_2 - r)]}{\cos[\alpha_2(r_2 - r_1)]}, \\ B_z(r) &= B_z(r_1) \frac{\sin[\alpha_2(r_2 - r)]}{\sin[\alpha_2(r_2 - r_1)]}, \end{aligned} \right\} \quad (17)$$

which requires that $\alpha_2(r_2 - r_1)$ satisfy

$$\tan[\alpha_2(r_2 - r_1)] = \frac{B_z(r_1)}{B_\phi(r_1)}. \quad (18)$$

In this case one has $B_\phi(r) = B_\phi(r_2)r_2/r$, $B_z = 0$ at $r > r_2$.

4. A multi- a model

An arbitrary solution to the nonlinear force-free equation with $a = \alpha(r)$ can be approximated by a multi- a model. The flux tube is modelled as n concentric rings with a constant within each ring.

Equation (3) gives

$$\mathbf{B}_{n-\alpha} = (0, a_i J_1(\alpha_i r) + b_i Y_1(\alpha_i r), a_i J_0(\alpha_i r) + b_i Y_0(\alpha_i r)) \quad (r_{i-1} < r \leq r_i), \quad (19)$$

with $i = 1, \dots, n$, $a_i = B_0$, $b_1 = 0$ and $r_0 = 0$. Continuity at each r_i yields equations for a_i and b_{i+1} , the analogues of (4). The enclosed current at r_i is required to fit some specified current profile. This reduces to $B_{n-\alpha, \phi} = f(\alpha_i, r_i)$, thus fixing one of α_i or r_i .

4.1. Fitting procedure

The procedure used to fit an n - a approximation to a known, well-behaved solution to the force-free equation is as follows. As an example, the test solution is taken to be

$$\left. \begin{aligned} \mathbf{B}_{\text{test 1}} &= \left(0, \frac{B_0 r / r_{\text{out}}}{1 + (r/r_{\text{out}})^2}, \frac{B_0}{1 + (r/r_{\text{out}})^2} \right), \\ \alpha_{\text{test 1}}(r) &= \frac{2}{r_{\text{out}} [1 + (r/r_{\text{out}})^2]}, \end{aligned} \right\} \quad (20)$$

where r_{out} is a measure of the radius of the tube. The current corresponding to this magnetic field is

$$I_{\text{test 1}}(r) = \frac{2\pi r_{\text{out}} B_0}{\mu_0} \left[1 - \frac{1}{1 + (r/r_{\text{out}})^2} \right]. \quad (21)$$

The flux tube defined by this solution has infinite radius, so it must be truncated at some finite radius to be used in a solar context. This is chosen to be at

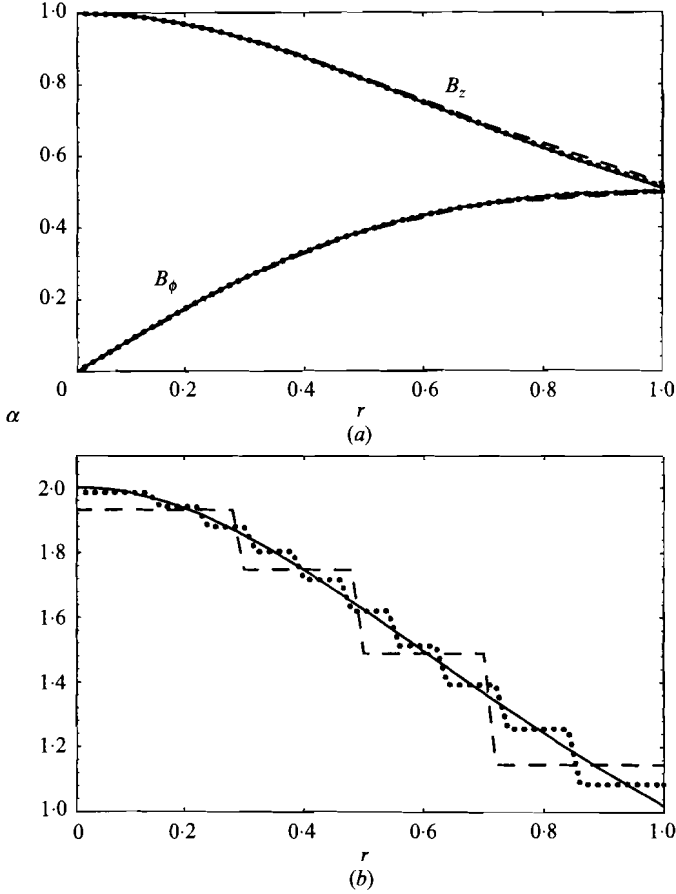


FIGURE 7. (a) B_ϕ and B_z as functions of radius: —, $B_{\text{test},\phi}$ for a well-behaved function (cf. (20)); ---, three-a approximation;, ten-a approximation. (b) As (a), but for \mathbf{a} .

$r_{\text{out}} = 1$. This in turn sets the outer radius of the n th concentric ring in the n - α approximation, that is, $r_n = r_{\text{out}}$. The magnitude of the magnetic field is arbitrary, so we set $a = B_0 = 1$. With these choices and with the various equations for fixing parameters discussed above, there are $n - 1$ free parameters, in this case chosen to be the r_i ($i = 1, \dots, n - 1$).

The first step in constructing the approximation is to choose a set of r_i . Then, working from the innermost ring outwards, a_i and b_i are written in terms of r_{i-1} , α_{i-1} and \mathbf{a} , where r_{i-1} and α_{i-1} are known. One then solves for the α_i using the condition that the current inside r_i in this approximation is equal to the current inside r_i for the trial solution. Using (6) and (21) yields

$$B_{n-\alpha,\phi}(\alpha_i r_i) = \frac{r_{\text{out}} B_0}{r_i} \left[1 - \frac{1}{1 + (r/r_{\text{out}})^2} \right]. \quad (22)$$

Once α_i is found, a_i and b_i are evaluated. This procedure is iterated until all the parameters have been found. The r_i ($i = 1, \dots, n - 1$) are then varied to find the best fit of $B_{n-\alpha,z}$ to $B_{\text{test},z}$.

The solutions B_ϕ , \mathbf{B} , and \mathbf{a} are plotted in figure 7, with the trial solution indicated by the solid line, the three-a approximation by the dashed line and

the ten-a: approximation by the dotted line. $B_{n-\alpha,\phi}(r_i)$ is the same as $B_{\text{test}1,\phi}(r_i)$ because of the constraint of equal enclosed currents at these points. Even with only three rings, $B_{n-\alpha,\phi}$ is a good fit. One needs more regions to produce a close fit to the z component than for the ϕ component. Nevertheless, this example shows that for well-behaved functions relatively few concentric rings are needed to give a good approximation to the trial solution.

4.2. Singular surface current

The n -a method can also be used to approximate a known solution in which the current density diverges at the edge of the tube. Such a solution is that used by Low (1993), which in cylindrical polar co-ordinates with z as the symmetry axis gives a second choice of test solution:

$$\left. \begin{aligned} B_{\text{test}2} &= (0, \frac{1}{8}\lambda^2 r, \lambda^2 [\frac{1}{8}(r_{\text{out}}^2 - r^2)]^{\frac{1}{2}}) \quad (r \leq r_{\text{out}}), \\ \alpha_{\text{test}2} &= \frac{1}{[2(r_{\text{out}}^2 - r^2)]^{\frac{1}{2}}}, \end{aligned} \right\} \quad (23)$$

where r_{out} is the outer edge of the tube and λ is a constant. The corresponding current is

$$I_{\text{test}2} = \frac{\pi\lambda^2 r^2}{2\mu_0}.$$

Since $a = B_0 = 1$, this fixes $\lambda = (2^{\frac{3}{2}}B_0/r_{\text{out}})^{\frac{1}{2}}$, and r_{out} is also set equal to unity.

The procedure is essentially the same as for a well-behaved solution, except for the outermost ring. For all the inner rings (19) is used as before, and the same method of solution is used to iteratively find the a_i ($i = 1, \dots, n-1$) and other parameters. given a set of r_i ($i = 1, \dots, n-1$). In the outermost ring the functional forms given in (17) and (18) are used for $B_{n-\alpha,\phi}$ and $B_{n-\alpha,z}$. That is,

$$\left. \begin{aligned} B_{n-\alpha,\phi}(r) &= B_{n-\alpha,\phi}(r_{n-1}) \frac{\cos[\alpha_n(r_n - r)]}{\cos[\alpha_n(r_n - r_{n-1})]} \quad (r_{n-1} \leq r \leq r_n), \\ B_{n-\alpha,z}(r) &= B_{n-\alpha,z}(r_{n-1}) \frac{\sin[\alpha_n(r_n - r)]}{\sin[\alpha_n(r_n - r_{n-1})]} \quad (r_{n-1} \leq r \leq r_n). \end{aligned} \right\} \quad (24)$$

Once the other parameters are known, a_n is found by setting $I_{n-\alpha}(r_n) = I_{\text{test}2}(r_n)$. One can invert (24) to find

$$\alpha_n = \frac{\arccos[(4/\lambda^2 r_n) B_{n-\alpha,\phi}(r_{n-1})]}{r_n - r_{n-1}}$$

The r_i ($i = 1, \dots, n-1$) are again varied to find the best fit of $B_{n-\alpha,z}$ to $B_{\text{test}2}$.

The solutions B_ϕ , B_z , and a are plotted in figure 8, with the trial solution indicated by the solid line, the three-a: approximation by the dashed line and the ten-a approximation by the dotted line. The same qualitative remarks can be made in this case of a divergent current density as are made for the well-behaved solution.

These examples establish that this method of approximation works well. It is straightforward to use it to construct piecewise-constant- a models to fit a given current profile whose associated magnetic fields are not known.

Force-free flux tubes

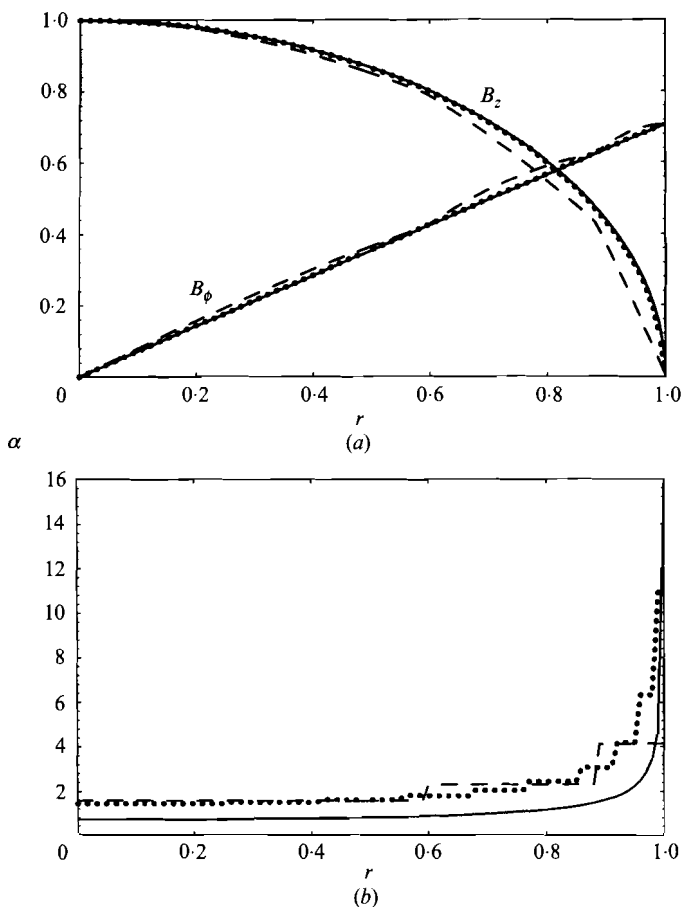


FIGURE 8. (a) B_ϕ and B_z as functions of radius: —, $B_{\text{test},\phi}$ for a solution with a singular surface current (cf. (23)); ---, three-a approximation; ·····, ten-a approximation. (b) As (a), but for α .

5. Discussion and conclusions

In summary, the main points made here are as follows.

(i) Flux tubes are classified here as current-neutralized if their exterior has $B_\phi = 0$, $B_z \neq 0$, and isolated current-carrying if their exterior has $B_\phi \neq 0$, $B_z = 0$.

(ii) A single-a model for a current-neutralized force-free flux tube involves a reverse-field pinch configuration, which has zero total magnetic flux. Such a model is unacceptable for a solar flux tube, which has a non-zero magnetic flux, but may be acceptable for an astrophysical jet (see e.g. Konigl & Choudhuri 1985).

(iii) A two-a model permits current neutralization with a non-zero magnetic flux. Several such models have been illustrated.

(iv) A single-a surface current layer may be constructed to satisfy either the boundary conditions $B_\phi = 0$, $B_z \neq 0$, or $B_\phi \neq 0$, $B_z = 0$ in the exterior region. For a thin surface current layer the solutions are given in terms of trigonometric functions (cf. (15) and (17)).

(v) An arbitrary force-free current profile (that is, arbitrary $\alpha(r)$) may be approximated by a multi- a model involving a sequence of concentric cylindrical shells with piecewise-constant a .

REFERENCES

- BRAY, R. J., CRAM, L. E., DURRANT, C. J. & LOUGHHEAD, R. E. 1991 *Plasma Loops in the Solar Corona*. Cambridge University Press.
- BROWNING, P. K., SAKURAI, T. & PRIEST, E. R. 1986 *Astron. Astrophys.* **158**, 217.
- CHIUDERI, C., EINAUDI, G., MA, S. S. & VAN HOVEN, G. 1980 *J. Plasma Phys.* **24**, 39.
- GOLD, T. & HOYLE, F. 1960 *Mon. Not. R. Astron. Soc.* **120**, 89.
- HEYVAERTS, J. & PRIEST, E. R. 1984 *Astron. Astrophys.* **137**, 63.
- KÖNIGL, A. & CHOUDHURI, A. R. 1985 *Astrophys. J.* **289**, 173.
- LOW, B. C. 1985 *Solar Phys.* **100**, 309.
- LOW, B. C. 1993 *Astrophys. J.* **409**, 798.
- LUST, R. & SCHLÜTER, A. 1954 *Z. Astrophys.* **34**, 263.
- NORMAN, C. A. & HEYVAERTS, J. 1983 *Astron. Astrophys.* **124**, L1.
- PARKER, E. N. 1979 *Cosmical Magnetic Fields*. Oxford University Press.
- PRIEST, E. R. 1982 *Solar Magnetohydrodynamics*. Reidel.
- TAYLOR, J. B. 1974 *Phys. Rev. Lett.* **33**, 1139.
- TAYLOR, J. B. 1986 *Rev. Mod. Phys.* **58**, 741.